Plant Physiology and Biochemistry 217 (2024) 109256

Contents lists available at ScienceDirect

Plant Physiology and Biochemistry

journal homepage: www.elsevier.com/locate/plaphy

CsUGT95B11 glycosylates quercetin to enhance resistance of tea plant (*Camellia sinensis*) to *Ectropis grisescens*

Hongrong Chen, Dahe Qiao, Lingling Tao, Songyan Huang, Hui Xie, Kelin Huang, Shengrui Liu, Junyan Zhu **, Chaoling Wei *

State Key Laboratory of Tea Plant Biology and Utilization/ Key Laboratory of Tea Biology and Tea Processing of Ministry of Agriculture/ Anhui Provincial Laboratory of Tea Plant Biology and Utilization/ Anhui Agricultural University, West 130 Changjiang Road, Anhui, 230036, China

ARTICLE INFO

Keywords:
Glycosyltransferase
Ectropis grisescens
Camellia sinensis
Quercetin glucoside
CsUGT95B11
Plant–herbivore interaction

ABSTRACT

Herbivore attack is a major type of biotic stress that greatly affects the development and quality of tea plant [*Camellia sinensis* (L) O. Kuntze]. Tea plant produces many glycosylated compounds that enhance resistance to herbivores. An example is quercetin, one of the major flavonols of tea plants, which was glycosylated to involve responses to various environmental stresses. However, not much is known about the biosynthesis of glycosylated quercetin derivatives in tea plant in response to herbivorous attack. Here, we found that *E. grisescens* attack significantly increased the contents of quercetin 3-*O*-glucoside and quercetin 7-*O*-glucoside in tea leaves, and exogenous application of these two compounds improved the *E. grisescens* resistance of tea plant. Integrated transcriptome and phylogenetic analyses identified *CsUGT95B11* gene, encoding a quercetin glycosyltransferase, which was upregulated in response to *E. grisescens* attack. Enzymatic assays showed that CsUGT95B11 preferentially glycosylated quercetin to produce quercetin 7-*O*-glucoside with a $k_{cat}{\cdot}K_m^{-1}$ value of 9655.52 M^{-1} s^{-1}. Subcellular localization analysis indicated that CsUGT95B11 was dispersed in the cytoplasm of *Nicotiana benthamiana* leaves and *Arabidopsis* protoplast. Suppression of *CsUGT95B11* reduced the quercetin glucoside content of tea leaves and impaired resistance of tea plant to *E. grisescens*. These results indicate that CsUGT95B11 is a quercetin glycosyltransferase that enhances resistance of tea plant to *E. grisescens*, providing insights into the mechanism of flavonol glycosylation regulating interactions between plants and herbivores.

1. Introduction

Herbivorous insects greatly affect crop yield and quality. In turn, plants have evolved diverse and complex mechanisms to detect and respond to insect feeding by regulating physiological and biochemical processes, as necessitated by their lack of mobility (Haukioja, 1991). Among the many factors that contribute to plant insect resistance are secondary metabolites, the main chemical basis of the resistance. Plant secondary metabolites typically do not serve as nutrients for insects; however, they can affect food selection, uptake, and utilization by insects, as well as those of other organisms (Mateos Fernández et al., 2022).

Flavonoids are important secondary metabolites and insect resistance compounds produced by plants (War et al., 2013). Flavonol biosynthesis was upregulated in response to herbivore feeding, suggesting that these metabolites were involved in herbivore resistance (Onkokesung et al., 2014). Flavonols may protect plants against herbivores and insects (Gautam et al., 2023). For instance, increased expression of genes related to the phenylpropanoid pathway leads to flavonol accumulation and enhanced insect resistance of tobacco (Misra et al., 2010). The mechanism of flavonoids in plant response to insect attack is unknown.

Glycosylation is a frequent modification of small-molecule compounds widely involved in plant growth, development, and defense responses (Wang and Hou, 2009). It is catalyzed by glycosyltransferases (GTs), a highly differentiated class of enzymes that transfer activated sugar molecules from the donor to the acceptor molecules to generate glycosidic compounds (Dewitte et al., 2016). GTs were classified into 115 protein families based on sequence homology, shared sequence, and catalytic specificity (http://www.cazy.org/GlycosylTransferases.html) (Ross et al., 2001). Over 100 uridine diphosphate (UDP) glycosyltransferase (UGT) genes were identified in *Arabidopsis*, over 180 and 200

* Corresponding author.
** Corresponding author.
E-mail address: weichl@ahau.edu.cn (C. Wei).

https://doi.org/10.1016/j.plaphy.2024.109256
Received 21 June 2024; Received in revised form 17 October 2024; Accepted 29 October 2024
Available online 31 October 2024

in grape and tea plant, respectively (Bowles et al., 2005; Offen et al., 2006; Hughes and Hughes, 2009). UGTs recognize and glycosylate various receptor molecules to produce numerous plant secondary metabolites (Hou et al., 2004) and are involved in plant defense and growth (Tognetti et al., 2010). For example, SfUGT33F28 affects maize resistance to the fall armyworm (Israni et al., 2022). Characterization of plant-specific UGTs and their mechanism of action in response to specific stresses is an on-going effort.

UGTs produce *O*-, *C*-, *N*-, and *S*-glucosides by acting on various glycosidic bonds (Dai et al., 2022). *O*-glucosides are the most common, whereas *N*- and *S*-glucosides are the least common. For example, AtUGT76C1 and AtUGT76C2 form *N*-glucosides with cytokinins as acceptor, whereas AtUGT73C1 and AtUGT73C5 form *O*-glucosides. *O*-glucosides are easier to store than *N*-glucosides (Hou et al., 2004). AtUGT74B1 catalyzes the formation of *S*-glucosides, whereas AtUGT73B4 catalyzes the formation of *C*-glucosides (Grubb et al., 2004; Langlois-Meurinne et al., 2005). Depending on the glycosylation site, plant flavonoid glycosyltransferases can be classified as 3-*O*-, 5-*O*-, or 7-*O*-glycosyltransferases (Veitch and Grayer, 2008; Dai et al., 2017). Among the *Arabidopsis* UGTs, 29 exhibit catalytic activity towards quercetin (Lim et al., 2004). Among them, 14 are catalytically active at only 1 hydroxylated site, 11 can glycosylate 2 hydroxylated sites, 3 recognize 3 hydroxylated sites, and only 1 glycosylates 4 hydroxylated sites (Lim et al., 2004). Most UGTs exhibit a strict regional selectivity. For example, AtUGT78D1 and AtUGT78D2 can only produce flavonol 3-*O*-glucosides (Mo et al., 2016), whereas WsGT can only catalyze the generation of 7-*O*-glucosides from lignans, apigenin, naringenin, genistein, and soy glucosides (Kumar et al., 2013). Multisite glycosylation is a rare function of UGTs. UGT74F1 from *Arabidopsis* glycosylates quercetin at the 3′-OH, 4′-OH, and 7-OH positions (Quiel and Bender, 2003), whereas UGT73C6 produces quercetin 3-*O*-glucoside, 7-*O*-glucoside, 3′-*O*-glucoside, and 4′-*O*-glucoside (Hou et al., 2004). Glycosides with different hydroxyl sites for resistance to herbivores in plants need to be further investigated.

Tea is regarded as one of the most popular nonalcoholic beverages globally. It is primarily processed from the tea leaves (Shi et al., 2011). The quality and yield of tea leaves are sensitive to herbivore attacks, and other biotic and abiotic stresses. Numerous characterized secondary metabolites were found to be involved in herbivore resistance of tea plant, such as flavonoids, caffeine, and terpenoids (Li et al., 2022). For example, quercetin in cotton reduces the survival rate of bollworms (Liu et al., 2015), and its derivative, quercetin 3-*O*-glucoside can enhance herbivore resistance in tea plant (Jing et al., 2023). Considering that glycosides in tea plant are characterized by multisite modification, which responds to fluctuating environmental stress (Zhao et al., 2017), the biosynthesis mechanism of quercetin glucoside and its biological function in response to herbivore feeding in tea plant are not yet understood.

Here, we aimed to investigate the enzymatic and biological functions of CsUGT95B11, a novel quercetin glycosyltransferase. We first observed that *E. grisescens* feeding increased quercetin glucoside content in tea leaves, and exogenous application of these two compounds improved the *E. grisescens* resistance of tea plant. The expression of *UGT95B11* was concomitant with a strong induction. The protein catalyzed the glycosylation of flavonols, with the highest affinity for quercetin of all substrates tested, and produced quercetin 3-*O*-glucoside and 7-*O*-glucoside. Suppression of *UGT95B11* expression in tea leaves led to a significant reduction of both quercetin glucoside content and tea plant resistance to *E. grisescens*. The current study thus revealed the key defensive role of quercetin glycosylation mediated by CsUGT95B11 in tea plant against *E. grisescens* and highlights the importance of multisite glycosylation of flavonoids in plant resistance to biotic stresses.

2. Materials and methods

2.1. Plant material

In this study, 2-year-old tea plants (*C. sinensis cv. Shuchazao*) were obtained from the Dechang Tea Garden (Shucheng, Anhui, China). The plants were grown in the same experimental field under natural light. They were selected based on consistent growth and the absence of pests or diseases. Indoor culture was conducted at 23 °C, with a light/dark photoperiod of 16 h of light and 8 h of darkness, and 65% humidity.

E. grisescens was captured and identified in the Dechang Tea Garden (Shucheng, Anhui, China). The insects were kept indoors, at 25 °C, with a light cycle comprising of 14 h of light and 10 h of darkness, and at 65% humidity. For the insect feeding experiments, the 3rd larvae were placed on the tea leaves to feed. The *E. grisescens* were removed after feeding on 1/3 of the tea leaves, the leaves were sampled at 3, 6, 9, 12, and 24 h. The control group consisted of untreated leaves that were sampled at the same time as the *E. grisescens*-consumed leaves. This treatment used clonal plants (Zhu et al., 2018).

MeJA was dissolved in Tween-20 and then diluted with pure water to a final concentration of 1 mM for MeJA and 0.05% for Tween-20. The MeJA solution was sprayed on the surface of tea leaves, and treatments were conducted for 3, 6, 9, 12, and 24 h, respectively. The leaves treated with 0.05% Tween-20 served as the control group. All treatments were performed in three biological replicates. The collected samples were immediately frozen in liquid nitrogen and stored at −80 °C until use (Zhu et al., 2024).

2.2. Transcriptome analysis

RNA-seq data of leaf samples from four stages (accession PRJNA901518) were analyzed as previously described. The clean RNA sequencing data from each sample were mapped to the tea plant genome using Tophat (v2.0.11) (Trapnell et al., 2009). The maximum alignment number for each read was set to 2.0, and the inner distance between mating pairs was set to 230 bp. The mapped reads were assembled with Cufflinks v.2.1.1 to generate a genome-based Cufflinks assembly. Default values were used for the remaining parameters. Based on gene length and numbers of fragments mapped to the corresponding genes, we calculated FPKM values, normalized using the Z-score in R Studio (Cole et al., 2012). For each comparison, genes with an adjusted $P \leq 0.05$ and fold change ≥ 2.00 were considered differentially expressed genes.

2.3. Chemicals and reagents

Quercetin, kaempferol, caffeic acid, prunetin, geranylin, delphinidin, cyanidin, farnesene, linalool, geraniol, methyl jasmonate, jasmonic acid, nerolidol, citronellol, erythromycin, basilene, benzyl alcohol, abscisic acid, farnesol, methyl salicylate, benzoic acid, 2-phenylethanol, quercetin 3-*O*-glucoside, and quercetin 7-*O*-glucoside were purchased from Sigma (MO, USA). Unless specified otherwise, UDP-glucose was obtained from Promega (Madison, USA).

2.4. RNA isolation and cDNA cloning

Total RNA was extracted from tea leaves using a Polysaccharide Polyphenol Plant RNA Extraction Kit (Novozymes, Nanjing, China) following the manufacturer's instructions. The extracted RNA samples were reverse-transcribed using a Prime Script 1st Strand cDNA Synthesis Kit (Takara, Japan) according to the manufacturer's instructions, and the resulting cDNA was used as a template for polymerase chain reaction (PCR) amplification. Specific primers were used to amplify full-length *CsUGT95B11* (Supplementary Table S1).

2.5. Phylogenetic tree construction

A phylogenetic tree was constructed using the neighbor-joining method in MEGA6.0 software based on the deduced amino acid sequences for the UGTs of interest, utilizing 342 UGT protein sequences to analyze the putative products of candidate genes with the following parameters: complete deletion, uniform rates, Poisson's model, and bootstrap method (1000 replicates).

2.6. Subcellular localization assays

CsUGT95B11 ORF was amplified without a stop codon using PCR, and the product was ligated with the pK7WGF2 vector using Gateway technology to construct a UGT95B11-GFP fusion protein under the control of the 35S promoter (Supplementary Table S1). The resultant pK7WGF2-UGT95B11 plasmid was used to transform *Agrobacterium* EHA105 Competent Cells (Weidi, Shanghai, China). Positive colonies were infiltrated with *Nicotiana benthamiana (N. benthamiana*). After 48 h of incubation, the infected leaves were collected and observed under a Lecia DMi8 confocal microscope (Lecia, Germany).

The recombinant plasmid was transformed into *Arabidopsis* protoplast and cultured overnight at 25 °C in the dark according to earlier reported protocol (Yoo et al., 2007). After 16 h of transformation, Green Fluorescent Protein (GFP) signal was observed using Lecia DMi8 confocal microscope (Lecia, Germany). Using ImageJ software (version 1.53a) for quantitative analysis of fluorescence data, the Pearson correlation coefficient was calculated to determine the subcellular colocalization of fluorescence signals in Arabidopsis protoplasts (Dunn et al.).

2.7. qRT-PCR analysis

Total RNA was extracted from tea plants using the method by our team (Zhu et al., 2024). Then, 1 μg of RNA was used for cDNA synthesis using the PrimeScrip RT Kit (Takara, Japan). The qRT-PCR procedure and reaction system were based on a method described earlier by our team (Zhu et al., 2024). The *CsGAPDH* gene was used as an internal control. cDNA amplification was performed using specific primers (Supplementary Table S1). The amplification efficiencies of all primers employed in the current study exhibited a range of 95%–105% (Bio-Red, USA). Relative gene expression was calculated using the $2^{-\triangle Ct}$ method, and statistical analysis was performed using DPS software.

2.8. Glucoside-fed tea plant experiment

Quercetin 3-*O*-glucoside, quercetin 7-*O*-glucoside, and a mixture of the two glucosides were each diluted with sterile water to a final concentration of 0.5 μg mL^{-1}. Tea plant branches were placed in centrifuge tubes filled with quercetin glucoside solution and incubated for 12 h at 25 °C and 65% relative humidity. The control group was tea plant branches treated with water under the same conditions. After treatment for 12 h, the samples were immediately observed for *E. grisescens* feeding.

2.9. Suppression of CsUGT95B11 expression in tea leaves treated with AsODN

Soligo software designed antisense oligonucleotide (*AsODN*) sequences were complementary to CsUGT95B11 using random oligonucleotides and sterilized water as controls (Dinc et al., 2011; Liu et al., 2018). Sequences were synthesized and purified using PAGE. *AsODN* and random oligonucleotides were diluted to a 100 μmol L^{-1} concentration. One bud and two leaves of tea branches were inserted into 1.5 mL tubes containing diluted primer liquid, and the tubes were sealed with sealing film. The branches were incubated in a growth chamber at 23 °C with 16 h of light and 8 h of darkness, and humidity was maintained at 65%. Samples were collected at 8, 12, and 24 h. RNA sample was extracted, and the optimal time was selected by quantitative expression analysis. Leaves with inhibited *CsUGT95B11* expression were used for *E. grisescens* feeding, and the weight of consumed leaves was recorded. In the feeding experiment with *E. grisescens*, we used two tea leaves as one biological replicate, conducting a total of four biological replicate experiments. Primer sequences and *AsODNs* used in this study are listed in Supplementary Table S1.

2.10. Heterologous expression and purification of CsUGT95 protein

The pMAL-c5x vector was double-cleaved with restriction endonucleases *Sal*I and *Eco*RI. Then, *CsUGT95B11* was ligated with the pMAL-c5x vector, using the ClonExpress II One-Step Cloning Kit (Vazyme, Nanjing, China). After confirming the correctness of the cloned fragment by sequencing, the resultant pMAL-C5X-UGT95B11 plasmid was used to transform *Escherichia coli* Rosetta (DE3) cells. Affinity purification of maltose-binding protein (MBP)–tagged recombinant protein was conducted using straight-chain amylose resin. For SDS-PAGE analysis, 3 mg of the recombinant protein was boiled for 10 min in a 5 × loading buffer (Sigma, USA) and analyzed on 12.5% SDS-PAGE gel (Yamei, Shanghai, China).

2.11. Enzymatic assays and analysis of kinetic parameters

For substrate screening, the reaction mixture contained 50 mM Tris-HCl buffer (pH 7.5), 10 mM dithiothreitol, 10% glycerol, 4 mM acceptor substrate, 250 mM UDP-glucose, and 1 μg purified CsUGT95B11 protein in 5 μL reaction volume. The reaction mixture was incubated at 30 °C for 30 min, and the reaction was stopped by adding an equal volume of the detection reagent. Three replicates of each experiment were performed.

The optimal pH range for the reaction was determined to be between 4.5 and 8.5, using MES (pH 4.5–6.5) and Tris-HCl (pH 6.5–8.5) buffers. The optimum temperature was determined in the range of 20–45 °C, at pH 7.5. The optimum reaction time was determined in the range of 10–60 min, at 40 °C and pH 7.5. The kinetic parameters of enzyme activity were determined under optimized conditions with eight different concentrations (from 1 to 1000 μM) of quercetin as the acceptor substrate (Zhao et al., 2020b).

2.12. Determination of quercetin glucoside content in enzymatic reaction

The reaction mixture (500 μL) contained 5 μg of purified CsUGT95B11 protein, 250 mM substrate, and 5 mM UDP-glucose. The reaction mixture was incubated at 40 °C for 1 h. The reaction was stopped by ultrasonication, after adding 500 μL of 100% ethyl acetate. The upper, organic solvent layer of the reaction solution was removed and dissolved by rotary evaporation with 100 μL of methanol/water (1:1, v/v). The reaction products were analyzed using high-performance liquid chromatography (HPLC) (Jing et al., 2019). For the analysis, a reversed-phase C_{18} column (2.6 μm, 100 × 4.6 mm), with a solvent flow rate of 1 mL min^{-1}, column temperature of 40 °C, and injection volume of 10 μL were used. The mobile phase solvent A was water containing 0.075% formic acid (v/v), and solvent B was 100% acetonitrile. The following elution program was used: 0 min 10% B, 0–5 min 10–25% B, 5–10 min 25–50% B, 10–17 min 50–80% B, 17–20 min 80–30% B, 20–21 min 30–10% B, and 20–22 min 10% B. UV spectra were recorded between 200 and 380 nm, with a simultaneous detection by diode array at 255 nm (Acquity Arc, Agilent, USA).

2.13. Metabolite analysis

To analyze metabolites in tea leaves after *E. grisescens* feeding, tea leaves were freeze-dried for 72 h and ground into a powder. Methanol (1 mL) was added to 50 mg of the powder and vortex-mixed for 1 min. Ultrasonic extraction was performed for 20 min, followed by centrifugation at 4 °C, 12,000 rpm for 15 min. The upper layer was collected and

extracted twice. The final solution was diluted 50 times in methanol and passed through a 0.22 μm filter membrane. Chloro-phenylalanine solution (1 μg mL^{-1}) was added as an internal standard, and the mixture was then analyzed by liquid chromatography–mass spectrometry (LC-MS), using a non-directed approach. The analysis was done using a reversed-phase C_{18} column (1.9 μm, 100 × 2.1 mm), at a flow rate of 0.2 mL min^{-1}, column temperature of 40 °C, and injection volume of 5 μL. The mobile phase solvent A was water containing 0.075% formic acid (v/v), and solvent B was 100% acetonitrile. The elution program was as follows: 0 min 0.1% B, 0–10 min 7% B, 10–22 min 7% B, 22–25 min 11% B, 25–30 min 12% B, 30–31 min 14% B, 31–43 min 35% B, 43–45 min 80% B, and 45–47 min 0.1% B.

2.14. Statistical analysis

Statistical analyses were performed using SigmaPlot 12.5 and Excel for one-way analysis of variance (ANOVA) with *t*-tests to determine the differences between groups and their statistical significance. All experiments were performed in triplicate, and the mean and standard deviation (SD) were calculated. Differences were considered statistically significant at $*P < 0.05$ and $**P < 0.01$.

3. Results

3.1. Induction of quercetin glucoside accumulation and CsUGT95B11 expression in tea leaves by E. grisescens feeding

To determine the effects of *E. grisescens* on tea plants, we analyzed different chemical compounds in tea plants exposed to *E. grisescens* feeding at five different time points (3, 6, 9, 12, and 24 h). Overall, we detected 155 compounds in tea leaves and noted significant changes in flavonoid content upon insect exposure (Supplementary Table S2). According to an earlier study, quercetin 3-*O*-glucoside mediates resistance to *E. grisescens.* We therefore investigated the accumulation of quercetin glucosides in the feeding leaves of *E. grisescens*. After *E. grisescens* exposure, we observed a significant accumulation of quercetin glucoside in the tea leaves. After 3 h of feeding, the leaves contained 2.1-times more total quercetin glucoside than that in the control (untreated) leaves (Fig. 1A). Specifically, quercetin 3-*O*-glucoside and 7-*O*-glucoside exhibited increases of 1.8- and 2.3-times, respectively, compared with that in the control leaves (Fig. 1B and C).

To determine the role of quercetin glucoside in tea plant response to *E. grisescens*, we fed the tea plants with quercetin 3-*O*-glucoside, quercetin 7-*O*-glucoside, and mixture of two glucosides, and then observed the feeding of *E. grisescens*. Tea shoots were soaked in different quercetin glucoside solutions for 12 h and then the leaves were fed to *E. grisescens* for 2 h. The results showed that the consumption of tea leaves fed with quercetin glucosides was significantly lower than that of the control group (Fig. 1D and E). These results suggest that quercetin glucosides served as defensive compound that improved the resistance of tea plant against *E. grisescens*.

To identify the UGTs involved in the biosynthesis of quercetin glucosides, we analyzed the transcript levels of putative UGTs in tea leaves at different time points after *E. grisescens* damage. We identified the three most divergent candidate genes among the UGT genes: *CSS0028084.1*, *CSS0033555.1*, and *CSS0039619.1* (*CsUGT95B11*). To

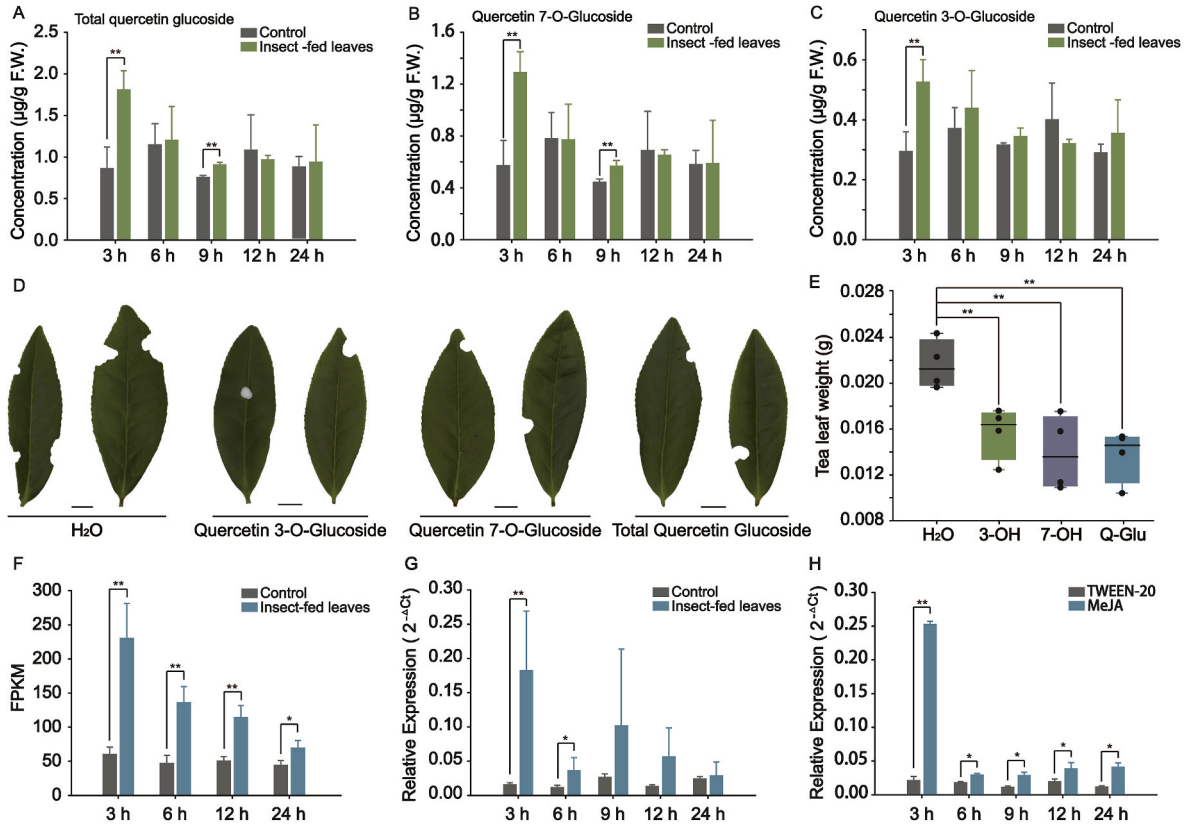

Fig. 1. Changes in quercetin glucoside content and *CsUGT95B11* expression in tea leaves after *E. grisescens* feeding. (A) Total quercetin glucoside, (B) quercetin 7-*O*-glucoside, and (C) quercetin 3-*O*-glucoside contents in tea leaves during *E. grisescens* feeding at five different time points. (D) Phenotypes of quercetin 3-*O*-glucoside (3-OH), quercetin 7-*O*-glucoside (7-OH), and total quercetin glucoside (Q-Glu) treated leaves after 2 h of *E. grisescens* feeding. (Scale = 1 cm). (E) Weight of tea leaves pre-treated as in (D) after 2 h of *E. grisescens* feeding. Error bars indicate SD ($n = 4$). ($*P<0.05$; $**P < 0.01$). (F) *CsUGT95B11* expression in response to *E. grisescens* feeding, based on transcriptome analysis. (G) qRT-PCR validation of *CsUGT95B11* expression in response to *E. grisescens* feeding. The data were normalized to *CsGAPDH* expression. (H) qRT-PCR analysis of *CsUGT95B11* expression in response to 1 mM MeJA treatment. The leaves treated with 0.05% Tween-20 served as the control group. The data represent the mean of three biological replicates. Error bars indicate SD ($n = 3$). $*P < 0.05$; $**P < 0.01$ (Student's *t*-test).

identify UGTs associated with the biosynthesis of quercetin glucosides, we analyzed the transcript levels of three candidate genes and correlated them with quercetin glucoside content. Among the three candidate genes, the expression of *CSS0039619.1* (*CsUGT95B11*, R = 0.86, *P* = 0.01) showed a stronger correlation with quercetin glucoside content than did *CSS0033555.1* (R = 0.79, *P* = 0.02) and *CSS0028084.1* (R = 0.35, *P* = 0.39) expression. Therefore, we selected the CsUGT95B11 gene with the strongest correlation for further experiments. Based on the transcriptome of tea leaves post-feeding with *E. grisescens*, *CsUGT95B11* was expressed at the highest level at the 3-h timepoint, and its expression declined from 6 to 24 h (Fig. 1F). qRT-PCR analysis confirmed that the expression of *CsUGT95B11* was the highest at 3 h after treatment, and 3.0-fold higher than that of the control (Fig. 1G). These findings suggest that *CsUGT95B11* is induced by *E. grisescens* feeding and is responsible for quercetin glucoside biosynthesis in tea plant.

On the basis of the important effect of JA signaling pathway on herbivore resistance of plant, we treated the tea plants with 1 mM MeJA as the JA derivative. The expression of *CsUGT95B11* was significantly upregulated, 12.5-fold, after 3 h of treatment (Fig. 1H). Collectively, these findings suggest that MeJA induces the expression of *CsUGT95B11*, which promotes the accumulation of quercetin glucosides in tea plant.

3.2. Identification and phylogenetic analysis of CsUGT95B11

We designed primers to amplify full-length *CsUGT95B11* cDNA from the tea plant genome. The full-length cDNA was 2169 bp in size, with an ORF (1563 bp) encoding a putative 56.23 kDa protein. We then constructed a phylogenetic tree for CsUGT95B11 using MEGA6.0 software. The previously identified UGTs with known functions formed 18 groups, A–R. CsUGT95B11 was assigned to Group Q along with CaUGT95B1 (Fig. 2). The UGT Nomenclature Committee designated this gene as UGT95B11 (https://labs.wsu.edu/ugt/).

Multiple sequence alignments of CsUGT95B11 homologs revealed conservation of the PSPG box in the UDP-binding domain (Fig. 3). The amino acid sequence of CsUGT95B11 contained an additional N-terminal region (79 aa) that was absent in its homologs and CaUGT95B1. Further, the alignment revealed that the amino acid sequence of

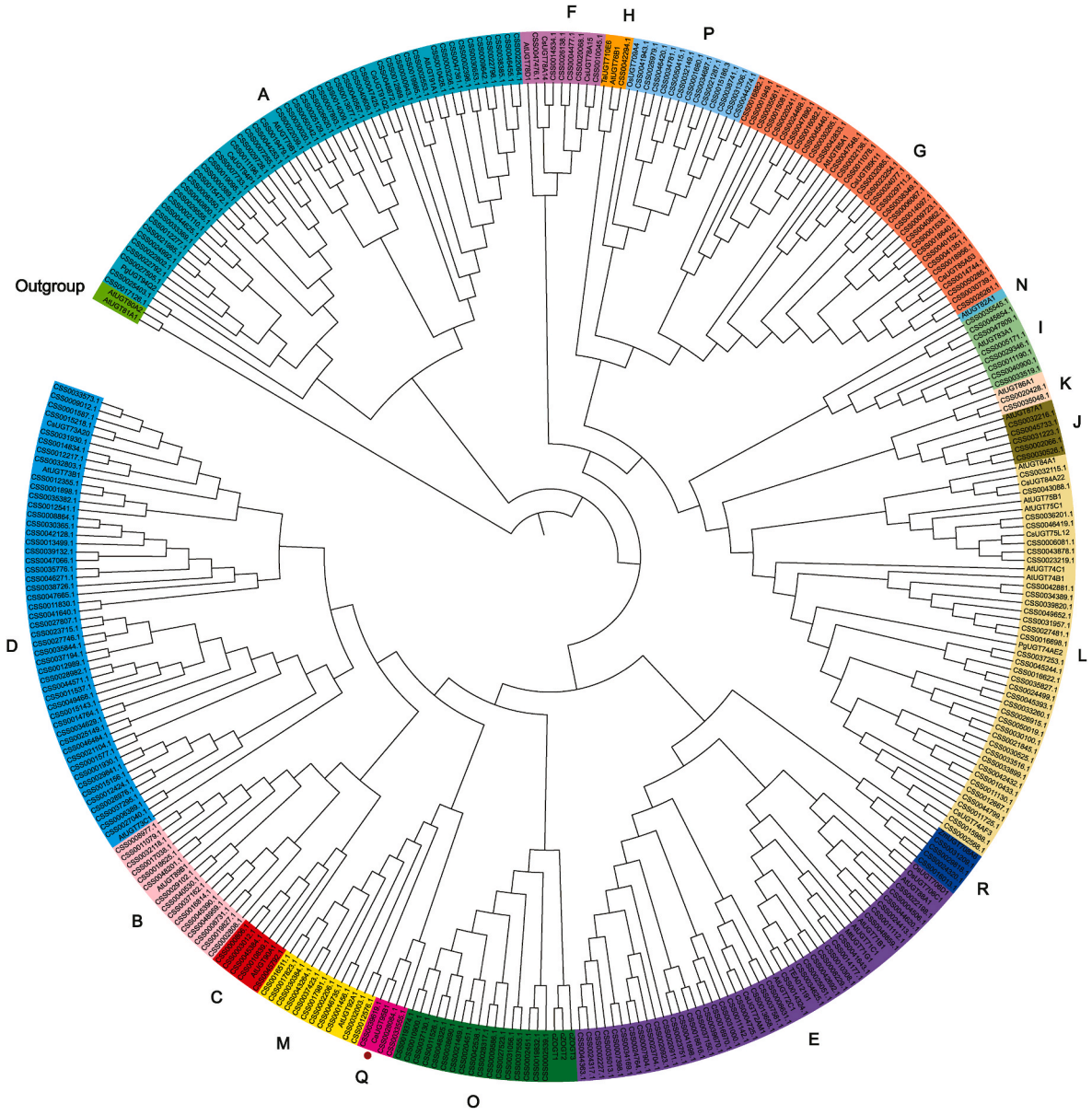

Fig. 2. Phylogenetic tree of plant UGTs. At, *Arabidopsis thaliana*; Ca, *Cicer arietinum*; cZO, cis-Zeatin-*O*-glucosyltransferase; Mt, *Medicago truncatula*; Os, *Oryza sativa* L.; Pg, *Panax ginseng*; Ta, *Triticum aestivum*; Zm, *Zea mays*.

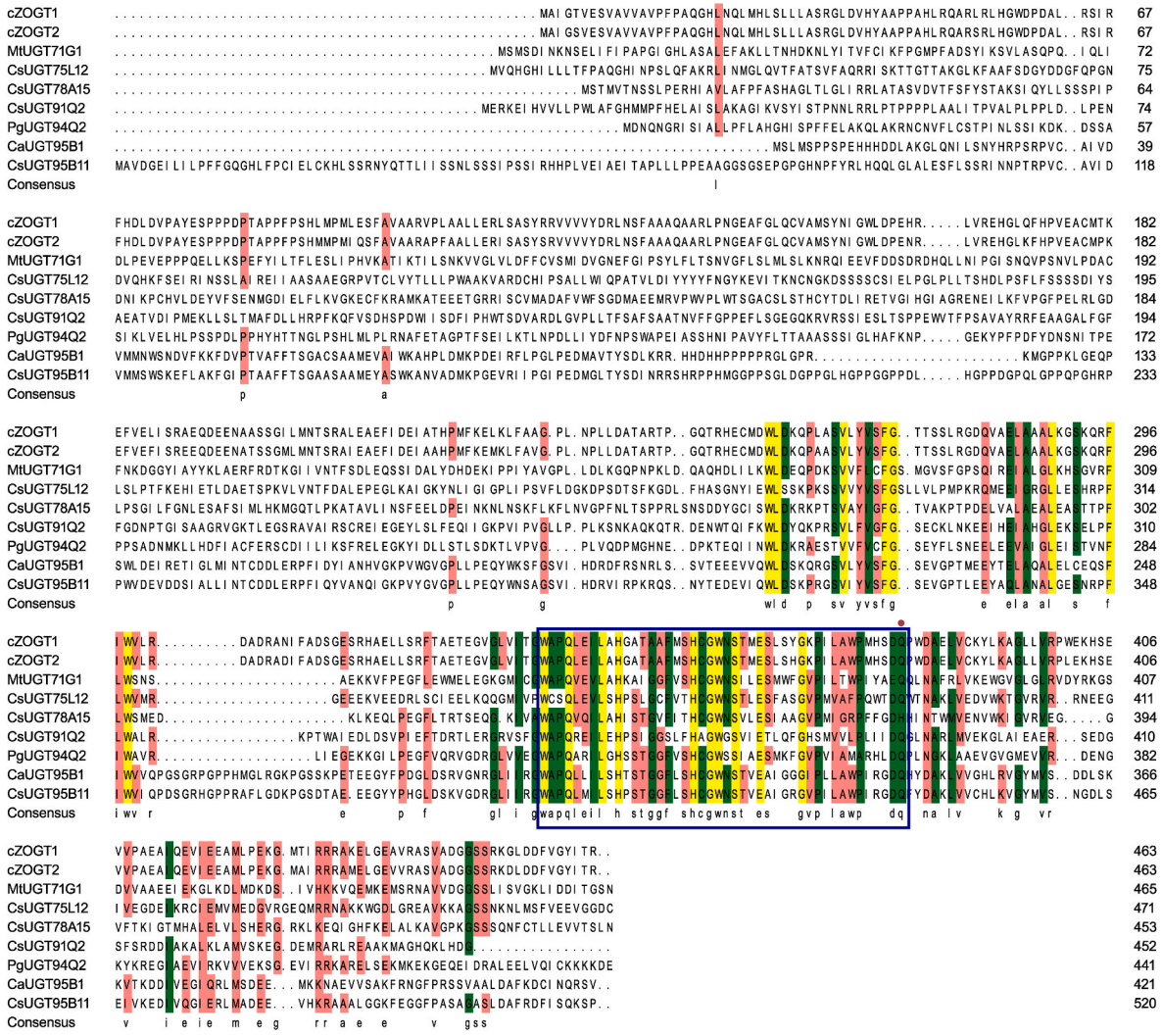

Fig. 3. Multiple alignment of deduced amino acid sequences of CsUGT95B11 and those of other UGTs. The UGT signature PSPG motif is enclosed in a blue box. The conserved residue in the sugar donor-binding site of CsUGT95B11 is denoted by a red dot. Ca, *Cicer arietinum*; Cs, *Camellia sinensis*; cZO, cis-Zeatin-*O*-glucosyltransferase; Mt, *Medicago truncatula*; Pg, *Panax ginseng*.

CsUGT95B11 shared 72.74% identity with that of CaUGT95B1. Finally, Q was the conserved residue in the sugar donor-binding site in CsUGT95B11 (Fig. 3).

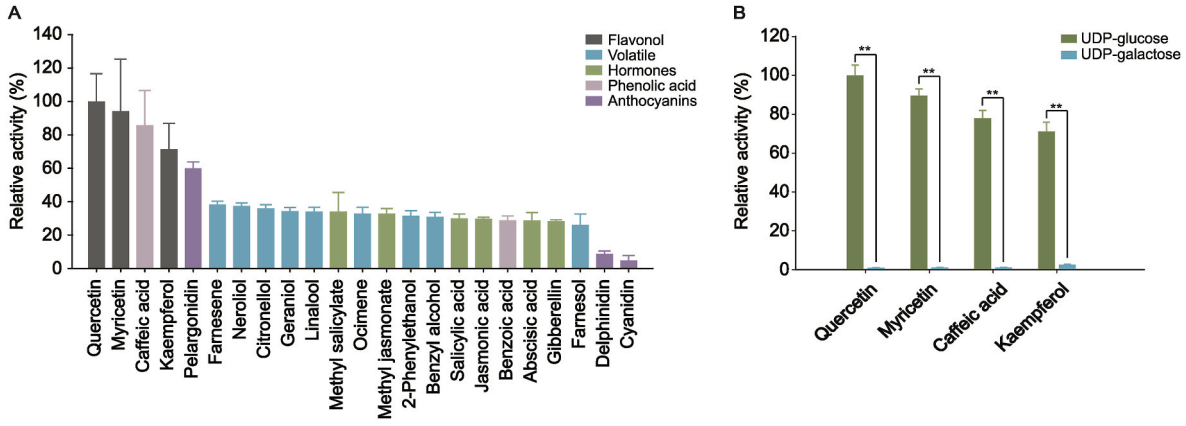

Fig. 4. Enzymatic activity of CsUGT95B11 in the presence of different sugar acceptors and donors. (A) Relative activity of CsUGT95B11 with 23 different compounds as the sugar acceptor, in a reaction with UDP-glucose as the sugar donor. (B) Relative activity of CsUGT95B11 with UDP-glucose or UDP-galactose as the donor. The data represent the mean of three biological replicates. Error bars indicate SD ($n = 3$). *$P < 0.05$; **$P < 0.01$ (Student's *t*-test).

3.3. *CsUGT95B11 preferably glycosylates quercetin to produce quercetin glucosides*

To determine the function of *CsUGT95B11*, we characterized the enzymatic activity of the encoded protein. We amplified the *CsUGT95B11* ORF from tea leaves using specific primers, and inserted the amplified sequence into a pMAL-c5x vector to generate the pMAL-c5x-CsUGT95B11 construct. The recombinant plasmid encoding CsUGT95B11 was then used to transform *E. coli* Rosetta (DE3) cells. The recombinant protein was then purified by affinity chromatography using a straight-chain amylose resin. The molecular weight of the purified recombinant protein was approximately 99 kDa, i.e., the expected sum of the molecular masses of MBP (42.5 kDa) and CsUGT95B11 (56.23 kDa). Next, we performed enzyme activity assays using flavonoid, volatile, and phenolic acid compounds as sugar acceptors. The analysis revealed that CsUGT95B11 exhibited the strongest catalytic activity with flavonoids among the compounds tested (Fig. 4A). Specifically, CsUGT95B11 exhibited the highest catalytic activity toward quercetin, followed by myricetin, caffeic acid, and kaempferol at 88.7%, 75.9%, and 71.1%, respectively, relative to that with quercetin.

The binding of sugar donors depends on the last amino acid in the conserved PSPG region of UGTs (Offen et al., 2006). In CsUGT95B11, the PSPG region ends with the amino acid Q (Fig. 3), suggesting that CsUGT95B11 can utilize UDP-glucose as a donor substrate. To explore the donor preference of CsUGT95B11, we tested UDP-glucose and UDP-galactose as the donor substrates, with quercetin as the acceptor substrate. We observed that CsUGT95B11 exhibited higher (100.5-fold) affinity for UDP-glucose than that for UDP-galactose (Fig. 4B). These results suggest that CsUGT95B11 uses quercetin and UDP-glucose as the preferred sugar acceptor and donor, respectively.

To explore the function of CsUGT95B11 on the quercetin glycosylation, we performed enzymatic reaction catalyzed by CsUGT95B11 with UDP-glucose and quercetin as the sugar donor and acceptor, respectively. The reaction products were identified and characterized using HPLC and LC-MS. HPLC analysis revealed that CsUGT95B11 catalyzed the formation of two glycosylation-derived products using quercetin as substrate; the retention times of quercetin 7-*O*-glucoside (4.833 min) and quercetin 3-*O*-glucoside (5.027 min) were comparative relative to that of standard, respectively (Fig. S1). Furthermore, using LC-MS analysis, the primary ion and characteristic fragment of quercetin 7-*O*-glucoside (m/z, 463.09 and 301.04) and quercetin 3-*O*-glucoside (m/z, 463.09 and 301.04) was also detected at different retention time in the enzymatic reaction mixture catalyzed by CsUGT95B11 (Fig. 5). Collectively, CsUGT95B11 catalyzes the glycosylation of quercetin at 7-OH and 3-OH *in vitro*, resulting in the production of quercetin 7-*O*-glucoside and quercetin 3-*O*-glucoside.

3.4. *Enzyme kinetics and subcellular localization of CsUGT95B11*

Considering the high enzymatic activity of CsUGT95B11 toward quercetin, myricetin, caffeic acid, and kaempferol (Fig. 4A), we further explored their enzymatic kinetics in presence of CsUGT95B11. First, the optimal pH, temperature, and reaction time for CsUGT95B11 was evaluated using quercetin, myricetin, caffeic acid, and kaempferol as sugar acceptor, respectively (Fig. 6A–C). Under the optimal reaction conditions, enzymatic kinetics of these four sugar acceptors were determined; the lowest K_m value (6.401 μM) was observed with quercetin (Fig. 6D), suggesting the high affinity of CsUGT95B11 toward quercetin than toward the other three sugar acceptors. Additionally, CsUGT95B11 exhibited higher enzymatic efficiency for quercetin than for the other substrates tested, with the $k_{cat}{\cdot}K_m^{-1}$ value of 9655.52 M^{-1} s^{-1}.

To examine subcellular localization of CsUGT95B11, we constructed expression vectors encoding CsUGT95B11-GFP and control (35S-GFP), and transiently expressed them in *N. benthamiana* leaves and *Arabidopsis* protoplast. Observation of GFP fluorescence signal in *N. benthamiana* leaves and *Arabidopsis* protoplasts showed that CsUGT95B11-GFP was localized exclusively in the cytoplasm, while 35S-GFP was diffusely present in the cytoplasm and nucleus (Fig. 7A and B and S2). Furthermore, the subcellular co-localization analysis showed the significantly

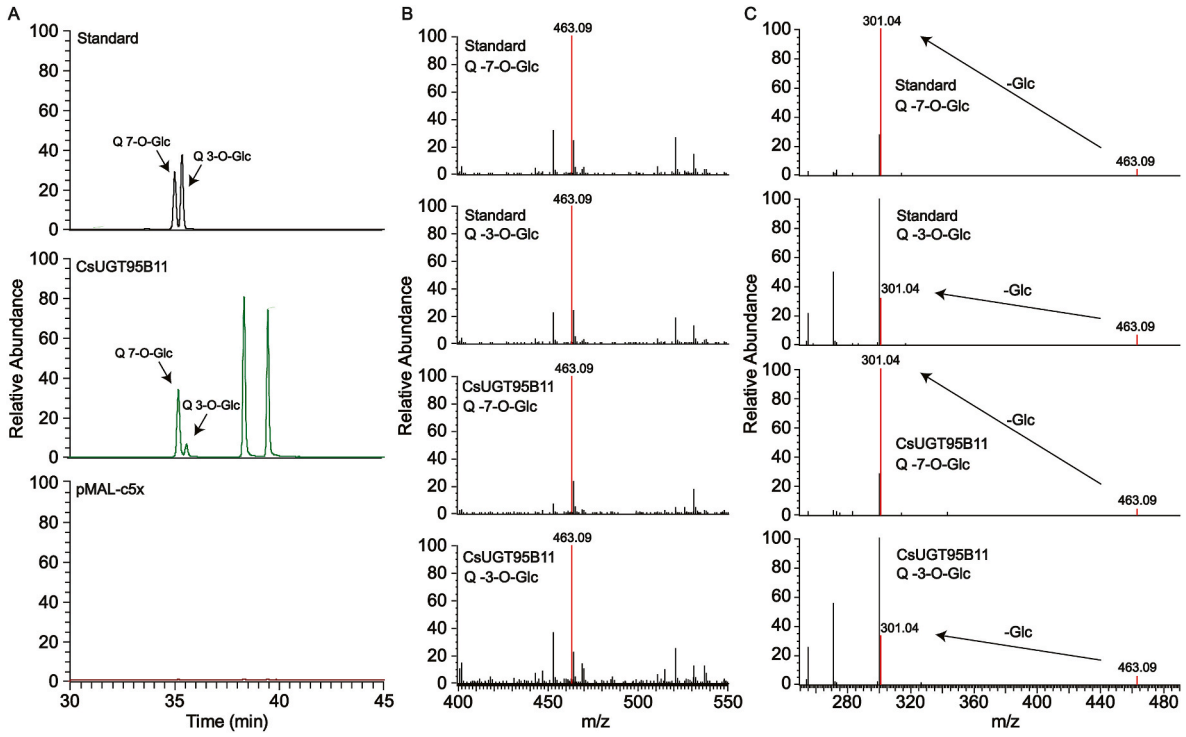

Fig. 5. CsUGT95B11 enzyme glycosylates quercetin to produce quercetin glucosides. (A) The products of the enzymatic reaction catalyzed by CsUGT95B11 were detected using LC-MS. The primary ion (B) and characteristic fragment (C) mass spectrometry profiles of quercetin glucoside standards and products of the enzymatic reaction catalyzed by CsUGT95B11.

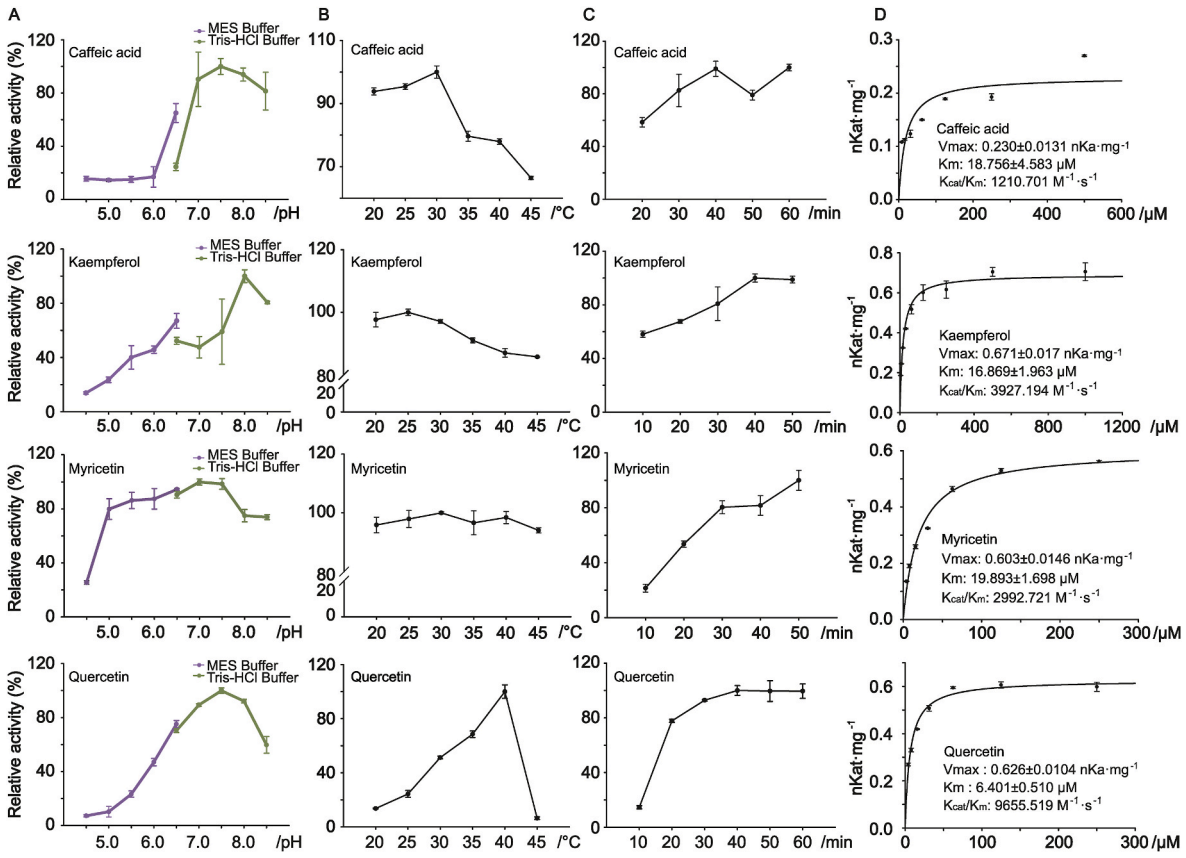

Fig. 6. Enzyme kinetics of CsUGT95B11 protein. Protein activity under different pH (A), temperature (B), and reaction time (C) conditions. (D) Kinetics of CsUGT95B11 using four different flavonoids as the sugar acceptor substrate and UDP-glucose as the sugar donor, under the optimized pH, time, and temperature conditions. Error bars indicate SD ($n = 3$).

negative relationship (Rr = −0.43, $P = 0.00594$) between GFP and chloroplast signal in *Arabidopsis* protoplast expressed CsUGT95B11-GFP construct (Fig. 7B and S2).

3.5. Reduction of tea plant resistance to E. grisescens by the suppression of CsUGT95B11 expression

To further investigate the role of *CsUGT95B11* in tea plant response to *E. grisescens*, we temporarily silenced *CsUGT95B11* expression in plants before exposure to the pest. We first designed three specific *AsODNs* based on the full-length *CsUGT95B11* sequence. We screened the gene silencing effectiveness after immersing tea plant shoots in different *AsODN* solutions for 12 h. Tea leaves treated with *AsODN_1* and *AsODN_2* effectively suppressed the expression of *CsUGT95B11* compared with that of the control. Among them, the *AsODN_2* was determined as the optimal AsODN probe used for suppression of *CsUGT95B11* expression, which resulted in the significant reductions of *CsUGT95B11* expression by 0.44-fold in *AsODN_2* treatment compared with that of the control (Fig. 8B). In another set of experiments, qRT-PCR revealed that *CsUGT95B11* expression was significantly suppressed after 12 and 24 h of treatment with *AsODN_2*. Further, after 12 h of treatment, *CsUGT95B11* expression was reduced by 0.76-fold in the leaves treated with *AsODN_2* compared with that in the control group (Fig. 8C). These results indicate that the expression of *CsUGT95B11* in tea leaves was efficiently suppressed by *AsODN_2*. Additionally, the quercetin glucoside content in CsUGT95B11-silenced tea was reduced by 0.09-fold compared with that of the control (Fig. 8D). Finally, to investigate the effect of quercetin glucosides on tea plant resistance to *E. grisescens*, we treated tea leaves with *AsODN* or sterilized water for 12 h and subjected them to *E. grisescens* feeding. After 2 h of feeding, the consumption of *CsUGT95B11*-silenced tea leaves was prominently higher than that of leaves treated with sterilized water (Fig. 8E and F). Summarily, CsUGT95B11 catalyzed the formation of quercetin glucosides, which enhanced tea plant resistance to *E. grisescens*.

4. Discussion

Herbivorous insects pose a major threat to the growth and production of tea plants. Several studies conducted on the physiological and biochemical responses of the tea plant to herbivores demonstrated that secondary metabolites related to herbivore-resistant defense, including phytohormones, flavonoids, and their glycoside derivatives, accumulate in large quantities in tea leaves (Jing et al., 2019). Simultaneously, the biosynthesis of numerous defensive compounds was modulated by the activation of jasmonic acid (JA) signaling in response to *E. grisescens* attack in tea plants, such as catechin, epicatechin, and epigallocatechin gallate (Zhang et al., 2020; Li et al., 2022). In our study, quercetin glucosides accumulated in response to *E. grisescens*, and the herbivore resistance of tea plant was reduced when quercetin glucosides were decreased (Fig. 8). In addition to the potential role of quercetin glucosides against herbivores, multiple studies have indicated that the accumulation of quercetin glucosides was associated with development and defense responses to UV light and pathogen infection in tea plant (Ohgami et al., 2014; Zhang et al., 2017; Jin et al., 2021). Furthermore, sensory analysis demonstrated that quercetin glucosides are the main astringent compound that affect the flavor formation of tea infusion (Cui et al., 2016). Therefore, considering the multifunctional role of quercetin glucosides in tea plants, effective manipulation of quercetin glucoside biosynthesis may be considered an efficient strategy that improves stress resistance and flavor of tea plant.

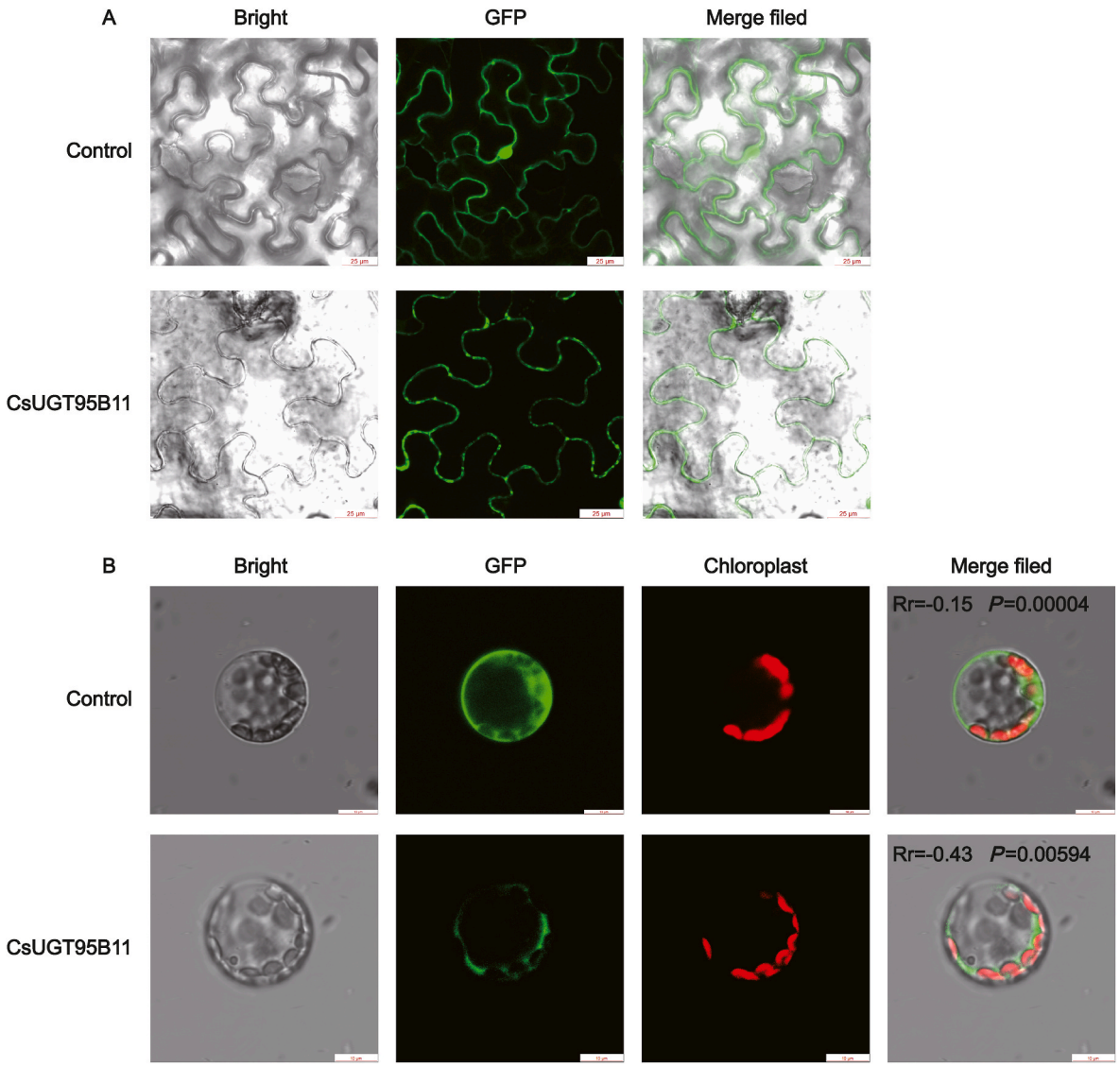

Fig. 7. Subcellular localization of CsUGT95B11-GFP protein. (A) GFP fluorescence signal of CsUGT95B11 protein in leaves of *N. benthamiana*. Scale = 25 μm. (B) GFP fluorescence signal of CsUGT95B11 protein in *Arabidopsis* protoplast ($n = 3$). Scale = 10 μm.

In plants, UGTs are characterized as the specialized enzymes that glycosylated numerous secondary metabolites to produce corresponding glucoside derivatives (Wilson and Tian, 2019). UGT families were subjected with obvious expansion and contraction, which can be classified into 17 subgroups during plant evolution and domestication (Caputi et al., 2012). In tea plants, 276 UGT genes were well identified and can be divided into 15 subgroups (Hoffmann et al., 2023); some of them were functionally characterized. For example, CsUGT78A4 and CsUGT71A59 belong to different subfamilies, which are collectively involved in cold response in tea plant (Zhao et al., 2020a, 2022), while UGT85A53 and UGT74Y1 are involved in the growth and development (Jing et al., 2020; Yang et al., 2023a). In our study, CsUGT95B11 was characterized as an induced glycosyltransferase in response to *E. grisescens* feeding, which was responsible for quercetin glucosides biosynthesis that contributed to herbivore resistance of tea plants (Figs. 1, 4, 5 and 8). Contrastingly, another member of B subgroup, CsUGT89AC1, also can catalyze the glycosylation of quercetin, while quercetin 3-*O*-glucoside was the exclusive enzymatic product (Jing et al., 2023). UGTs are considered the classical gene family in which members undergo sub-functionalization, neofunctionalization, and non-functionalization to adapt to the variable environmental stresses (Griesser et al., 2008). For example, VaUGT38 was able to glycosylate kaempferol to produce 3-*O*-glucoside and 7-*O*-glucoside, whereas VaUGT40 only produced 7-*O*-glucoside; further, reportedly, its multisite glycosylation property contributes to the adaptation of *Vernonia amygdalina* to a wide range of environments (Huo et al., 2021). Therefore, compared with the exclusive enzymatic function of CsUGT89AC1, whether the dual-functional CsUGT95B11 plays a predominant role in herbivore resistance in tea plant remains to be investigated.

Glycosylation of flavonoid compounds can occur at the 3, 5, 7, 3′ or 4′-site hydroxyl groups of the phenylpropanoid ring, respectively, or at multiple hydroxyl sites simultaneously (Kumar et al., 2013). A few UGTs that catalyze multiple-site glycosylation performing diverse biological functions in response to environmental stresses were identified (Griesser et al., 2008), such as the glycosylation of the quercetin with four different hydroxyl groups. Suppression of *GSA1* reduced quercetin 7-*O*-glucoside content, which attenuated the defense response to abiotic stresses in rice (Dong et al., 2020). NtUGT108 and NtUGT195 involved in the cold and drought response through glycosylating quercetin to produce quercetin 4-*O*-glucoside and 3-*O*-glucoside in *Nicotiana benthamiana* (Yang et al., 2023b). In our study, although quercetin 7-*O*-glucoside was higher than that of quercetin 3-*O*-glucoside catalyzed by CsUGT95B11 in tea leaves fed by the *E. grisescens* (Fig. 1B and C and 5), collectively improved the herbivore resistance of tea plant. It was

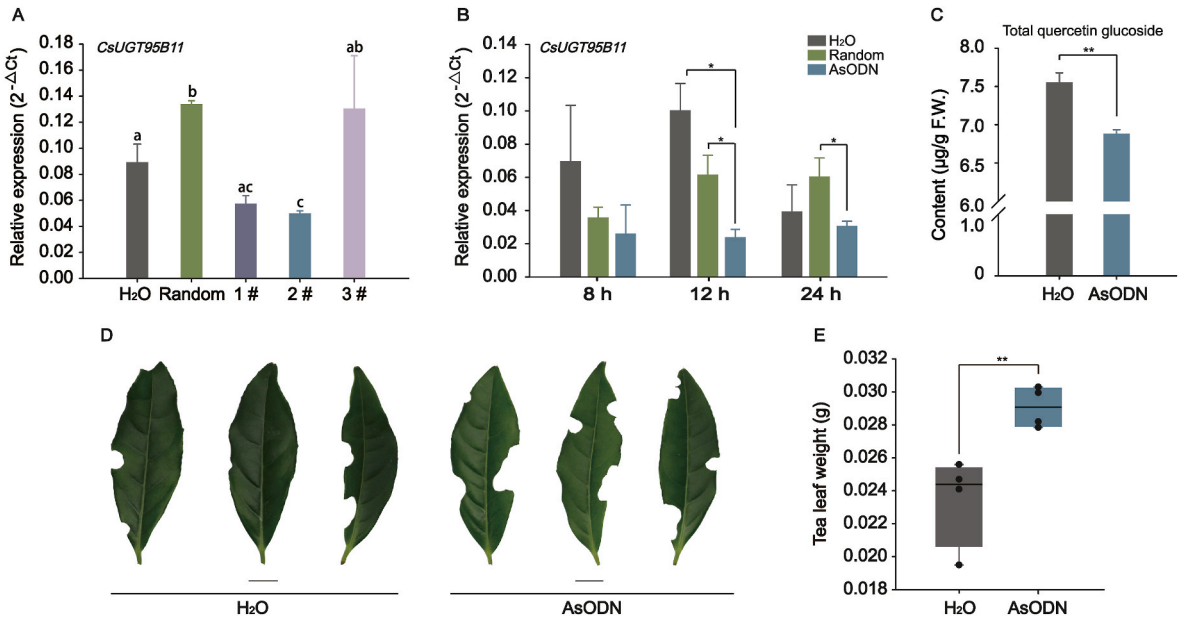

Fig. 8. Effect of CsUGT95B11 on quercetin glucoside biosynthesis and herbivore resistance of tea plant. (A) Relative expression of *CsUGT95B11* in tea leaves treated with three different AsODNs. Error bars indicate SD ($n = 3$). (*$P < 0.05$; **$P < 0.01$). (B) Relative expression of *CsUGT95B11* in tea leaves treated with sterilized water, random oligonucleotide, or anti-sense oligonucleotide (*AsODN_2*). H_2O, sterilized water treatment; Random, random oligonucleotide treatment. Error bars indicate SD ($n = 3$). (*$P < 0.05$; **$P < 0.01$). (C) Content of quercetin glucoside in leaves treated with sterilized water and *AsODN_2* for 12 h. Error bars indicate SD ($n = 3$). (*$P < 0.05$; **$P < 0.01$). (D) Phenotype of sterilized water- and AsODN-treated leaves after 2 h of *E. grisescens* feeding. Scale = 1 cm. (E) Weight of tea leaves pre-treated as in (D) after 2 h of *E. grisescens* feeding. Error bars indicate SD ($n = 4$). (*$P < 0.05$; **$P < 0.01$).

notably that there was no significant difference on defensive effect between quercetin 7-*O*-glucoside and quercetin 3-*O*-glucoside in response to the *E. grisescens* feeding (Fig. 1D and E). These results triggered us another question needed to explore in the future work, that what the biological function of quercetin 7-*O*-glucoside and quercetin 3-*O*-glucoside during environmental fluctuations in tea plant.

Summarily, we identified a CsUGT95B11 glycosyltransferase that was induced in response to *E. grisescens* feeding, and CsUGT95B11 preferentially glycosylated quercetin to produce quercetin 7-*O*-glucoside and quercetin 3-*O*-glucoside, thus being associated with the enhanced resistance of tea plants against *E. grisescens* feeding (Fig. 9). This finding advances our understanding of the mechanisms underpinning tea plant defenses against herbivores and provides insights into molecular breeding to enhance tea plant resistance to *E. grisescens*.

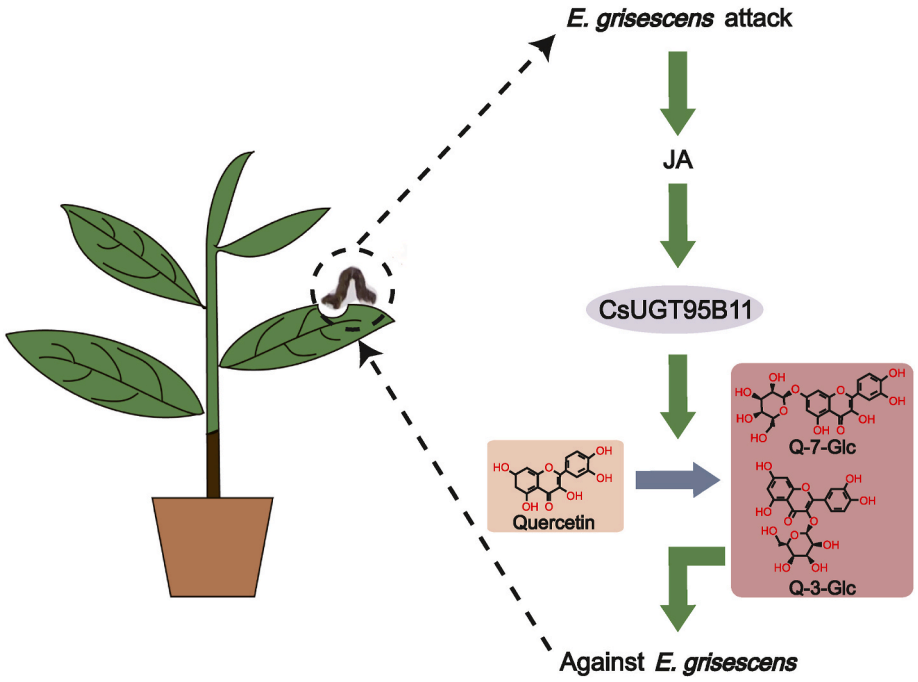

Fig. 9. Schematic model of CsUGT95B11-regulated biosynthesis of quercetin glucosides to enhance the resistance of tea plants against *E. grisescens*. *E. grisescens* attack induced the accumulation of JA in tea leaves. Increased JA production activates the expression of *CsUGT95B11* to accelerate the formation of quercetin glucosides, enhancing resistance of tea plants to *E. grisescens*.

Author contributions

Hongrong Chen: Writing – original draft, Visualization, Investigation, Formal analysis, Conceptualization. Dahe Qiao: Visualization, Investigation, Formal analysis. Lingling Tao: Formal analysis. Songyan Huang: Investigation, Formal analysis. Hui Xie: Data curation. Kelin Huang: Data curation. Shengrui Liu: Resources. Junyan Zhu: Writing – review & editing, Resources, Conceptualization. Chaoling Wei: Writing – original draft, Visualization, Funding acquisition, Conceptualization.

Declaration of competing interest

The authors declare that they have no known competing financial interests or personal relationships that could have appeared to influence the work reported in this paper.

Acknowledgements

This study was supported by the National Natural Science Foundation of China (Grant Numbers U20A2045 and 32202542), the National Joint Project of Tea Plant Breeding (GJCSYZLHGG-10), the Project of Science and Technology of Yunnan Province (Grant No. 202102AE090038), and the Project of Tea Plant Germplasm Resource Garden in Anhui.

Appendix A. Supplementary data

Supplementary data to this article can be found online at https://doi.org/10.1016/j.plaphy.2024.109256.

Data availability

Data will be made available on request.

References

Bowles, D., Isayenkova, J., Lim, E.K., Poppenberger, B., 2005. Glycosyltransferases: managers of small molecules. Curr. Opin. Plant Biol. 8, 254–263. https://doi.org/10.1016/j.pbi.2005.03.007.

Caputi, L., Malnoy, M., Goremykin, V., Nikiforova, S., Martens, S., 2012. A genome-wide phylogenetic reconstruction of family 1 UDP-glycosyltransferases revealed the expansion of the family during the adaptation of plants to life on land. Plant J. 69, 1030–1042. https://doi.org/10.1111/j.1365-313X.2011.04853.x.

Cole, T., Adam, R., Loyal, G., Geo, P., Daehwan, K., Kelley, D.R., Pimentel, H., Salzberg, S., Rinn, J., Pachter, L., 2012. Differential gene and transcript expression analysis of RNA-seq experiments with TopHat and cufflinks. Nat. Protoc. 7, 562–578. https://doi.org/10.1038/nprot1014-2513a.

Cui, L., Yao, S., Dai, X., Yin, Q., Liu, Y., Jiang, X., Wu, Y., Qian, Y., Pang, Y., Gao, L., Xia, T., 2016. Identification of UDP-glycosyltransferases involved in the biosynthesis of astringent taste compounds in tea (*Camellia sinensis*). J. Exp. Bot. 67, 2285–2297. https://doi.org/10.1093/jxb/erw053.

Dai, X., Shi, X., Yang, C., Zhao, X., Zhuang, J., Liu, Y.-J., Gao, L., Xia, T., 2022. Two UDP-glycosyltransferases catalyze the biosynthesis of bitter flavonoid 7-O-neohesperidoside through sequential glycosylation in tea plants. J. Agric. Food Chem. 70, 2354–2365. https://doi.org/10.1021/acs.jafc.1c07342.

Dai, X., Zhuang, J., Wu, Y., Wang, P., Zhao, G., Liu, Y., Jiang, X., Gao, L., Xia, T., 2017. Identification of a flavonoid glucosyltransferase involved in 7-OH site glycosylation in tea plants (*Camellia sinensis*). Sci. Rep. 7, 5926. https://doi.org/10.1038/s41598-017-06453-z.

Dewitte, G., Walmagh, M., Diricks, M., Lepak, A., Gutmann, A., Nidetzky, B., Desmet, T., 2016. Screening of recombinant glycosyltransferases reveals the broad acceptor specificity of stevia UGT-76G1. J. Biotechnol. 233, 49–55. https://doi.org/10.1016/j.jbiotec.2016.06.034.

Dinc, E., Toth, S.Z., Schansker, G., Ayaydin, F., Kovacs, L., Dudits, D., Garab, G., Bottka, S., 2011. Synthetic antisense oligodeoxynucleotides to transiently suppress different nucleus- and chloroplast-encoded proteins of higher plant chloroplasts. Plant Physiol. 157, 1628–1641. https://doi.org/10.1104/pp.111.185462.

Dong, N.Q., Sun, Y.W., G, T., S, C.L., Zhang, Y.M., Kan, Y., Xiang, Y.H., Zhang, H., Yang, Y.B., Li, Y.C., Zhao, H.Y., Yu, H.X., Lu, Z.Q., Wang, Y., Ye, W.W., Shan, J.X., Lin, H.X., 2020. UDP-glucosyltransferase regulates grain size and abiotic stress tolerance associated with metabolic flux redirection in rice. Nat. Commun. 11, 2629. https://doi.org/10.1038/s41467-020-16403-5.

Dunn, K. W., Kamocka, M. M., and McDonald J. H., A practical guide to evaluating colocalization in biological microscopy. American Journal of Physiology-Cell Physiology, 300, C723-C742. https://doi.org/10.1152/ajpcell.00462.2010.

Gautam, H., Sharma, A., Trivedi, P.K., 2023. The role of flavonols in insect resistance and stress response. Curr. Opin. Plant Biol. 73, 102353. https://doi.org/10.1016/j.pbi.2023.102353.

Griesser, M., Vitzthum, F., Fink, B., Bellido, M.L., Raasch, C., Munoz-Blanco, J., Schwab, W., 2008. Multi-substrate flavonol O-glucosyltransferases from strawberry (*Fragaria*×*ananassa*) achene and receptacle. J. Exp. Bot. 59, 2611–2625. https://doi.org/10.1093/jxb/ern117.

Grubb, C.D., Zipp, B.J., Ludwig-Muller, J., Masuno, M.N., Molinski, T.F., Abel, S., 2004. *Arabidopsis* glucosyltransferase UGT74B1 functions in glucosinolate biosynthesis and auxin homeostasis. Plant J. 40, 893–908. https://doi.org/10.1111/j.1365-313X.2004.02261.x.

Haukioja, E., 1991. Induction of defenses in trees. Annu. Rev. Entomol. 36, 25–42. https://doi.org/10.1146/annurev.en.36.010191.000325.

Hoffmann, T.D., Kurze, E., Liao, J., Hoffmann, T., Song, C., Schwab, W., 2023. Genome-wide identification of UDP-glycosyltransferases in the tea plant (*Camellia sinensis*) and their biochemical and physiological functions. Front. Plant Sci. 14, 1191625. https://doi.org/10.3389/fpls.2023.1191625.

Hou, B., Lim, E.K., Higgins, G.S., Bowles, D.J., 2004. N-glucosylation of cytokinins by glycosyltransferases of *Arabidopsis thaliana*. J. Biol. Chem. 279, 47822–47832. https://doi.org/10.1074/jbc.m409569200.

Hughes, J., Hughes, M.A., 2009. Multiple secondary plant product UDP-glucose glucosyltransferase genes expressed in cassava (*Manihot esculenta Crantz*) cotyledons. DNA Sequence 5, 41–49. https://doi.org/10.3109/10425179409039703.

Huo, K., Chen, Y., Sui, L., Wang, Y., Fu, Y., Pei, X., Niu, J., 2021. Transient expression and enzymatic assay identified uridine-diphosphate glucosyltransferases related to flavonoid glycosylation in *Vernonia amygdalina* leaves. Ind. Crop. Prod. 172, 114005. https://doi.org/10.1016/j.indcrop.2021.114005.

Israni, B., Luck, K., Römhild, S.C.W., Raguschke, B., Wielsch, N., Hupfer, Y., Reichelt, M., Svatoš, A., Gershenzon, J., Vassão, D.G., 2022. Alternative transcript splicing regulates UDP-glucosyltransferase-catalyzed detoxification of DIMBOA in the fall armyworm (*Spodoptera frugiperda*). Sci. Rep. 12, 10343. https://doi.org/10.1038/s41598-022-14551-w.

Jin, J., Lv, Y.-Q., He, W.-Z., Li, D., Ye, Y., Shu, Z.-F., Shao, J.-N., Zhou, J.-H., Chen, D.-M., Li, Q.-S., Ye, J.-H., 2021. Screening the key region of sunlight regulating the flavonoid profiles of young shoots in tea plants (*Camellia sinensis L.*) based on a field experiment. Molecules 26, 7158. https://doi.org/10.3390/molecules26237158.

Jing, T., Du, W., Qian, X., Wang, K., Luo, L., Zhang, X., Deng, Y., Li, B., Gao, T., Zhang, M., Guo, D., Jiang, H., Liu, Y., Schwab, W., Sun, X., Song, C., 2023. UGT89AC1-mediated quercetin glucosylation is induced upon herbivore damage and enhances *Camellia sinensis* resistance to insect feeding. Plant Cell Environ. 47, 682–697. https://doi.org/10.1111/pce.14751.

Jing, T., Zhang, N., Gao, T., Wu, Y., Zhao, M., Jin, J., Du, W., Schwab, W., Song, C., 2020. UGT85A53 promotes flowering via mediating abscisic acid glucosylation and FLC transcription in *Camellia sinensis*. J. Exp. Bot. 71, 7018–7029. https://doi.org/10.1093/jxb/eraa373.

Jing, T., Zhang, N., Gao, T., Zhao, M., Jin, J., Chen, Y., Xu, M., Wan, X., Schwab, W., Song, C., 2019. Glucosylation of (Z)-3-hexenol informs intraspecies interactions in plants: a case study in *Camellia sinensis*. Plant Cell Environ. 42, 1352–1367. https://doi.org/10.1111/pce.13479.

Kumar, R.J.S., Ruby, Singh, S., Sonawane, P.D., Vishwakarma, R.K., Khan, B.M., 2013. Functional characterization of a glucosyltransferase specific to flavonoid 7-*O*-glucosides from *Withania somnifera*. Plant Mol. Biol. Rep. 31, 1100–1108. https://doi.org/10.1007/s11105-013-0573-4.

Langlois-Meurinne, M., Gachon, C.M.M., Saindrenan, P., 2005. Pathogen-responsive expression of glycosyltransferase genes UGT73B3 and UGT73B5 Is necessary for resistance to *Pseudomonas syringae* pv *tomato* in *Arabidopsis*. Plant Physiol. 139, 1890–1901. https://doi.org/10.1104/pp.105.067223.

Li, X., Zhang, J., Lin, S., Xing, Y., Zhang, X., Ye, M., Chang, Y., Guo, H., Sun, X., 2022. (+)-Catechin, epicatechin and epigallocatechin gallate are important inducible defensive compounds against Ectropis grisescens in tea plants. Plant Cell Environ. 45, 496–511. https://doi.org/10.1111/pce.14216.

Lim, E.K., Ashford, D.A., Hou, B.-k., Jackson, R.G., Bowles, D.J., 2004. *Arabidopsis* glycosyltransferases as biocatalysts in fermentation for regioselective synthesis of diverse quercetin glucosides. Biotechnol. Bioeng. 87, 623–631. https://doi.org/10.1002/bit.20154.

Liu, D., Yuan, Y., Li, M., Qiu, X., 2015. Effects of dietary quercetin on performance and cytochrome P450 expression of the cotton bollworm, *Helicoverpa armigera*. Bull. Entomol. Res. 105, 771–777. https://doi.org/10.1017/s0007485315000760.

Liu, G.F., Liu, J.J., He, Z.R., Wang, F.M., Yang, H., Yan, Y.F., Gao, M.J., Gruber, M., Wan, X.C., Wei, S., 2018. Implementation of CsLIS/NES in linalool biosynthesis involves transcript splicing regulation in *Camellia sinensis*. Plant Cell Environ. 41, 176–186. https://doi.org/10.1111/pce.13080.

Mateos Fernández, R., Petek, M., Gerasymenko, I., Juteršek, M., Baebler, Š., Kallam, K., Moreno Giménez, E., Gondolf, J., Nordmann, A., Gruden, K., Orzaez, D., Patron, N.J., 2022. Insect pest management in the age of synthetic biology. Plant Biotechnol. J. 20, 25–36. https://doi.org/10.1111/pbi.13685.

Misra, P., Pandey, A., Tiwari, M., Chandrashekar, K., Sidhu, O.P., Asif, M.H., Chakrabarty, D., Singh, P.K., Trivedi, P.K., Nath, P., Tuli, R., 2010. Modulation of transcriptome and metabolome of *Tobacco* by *Arabidopsis* transcription factor, AtMYB12, leads to insect resistance. Plant Physiol. 152, 2258–2268. https://doi.org/10.1104/pp.109.150979.

Mo, T., Liu, X., Liu, Y., Wang, X., Zhang, L., Wang, J., Zhang, Z., Shi, S., Tu, P., 2016. Expanded investigations of the aglycon promiscuity and catalysis characteristic of flavonol 3-O-rhamnosyltransferase AtUGT78D1 from *Arabidopsis thaliana*. RSC Adv. 6, 84616–84626. https://doi.org/10.1039/C6RA16251G.

Offen, W., Martinez-Fleites, C., Yang, M., Kiat-Lim, E., Davis, B.G., Tarling, C.A., Ford, C. M., Bowles, D.J., Davies, G.J., 2006. Structure of a flavonoid glucosyltransferase reveals the basis for plant natural product modification. EMBO J. 25, 1396–1405. https://doi.org/10.1038/sj.emboj.7600970.

Ohgami, S., Ono, E., Toyonaga, H., Watanabe, N., Ohnishi, T., 2014. Identification and characterization of (*Camellia sinensis*) glucosyltransferase, UGT73A17: a possible role in flavonol glucosylation. Plant Biotechnol. 31, 573–578. https://doi.org/10.5511/plantbiotechnology.14.1027a.

Onkokesung, N., Reichelt, M., van Doorn, A., Schuurink, R.C., van Loon, J.J.A., Dicke, M., 2014. Modulation of flavonoid metabolites in Arabidopsis thaliana through overexpression of the MYB75 transcription factor: role of kaempferol-3,7-dirhamnoside in resistance to the specialist insect herbivore *Pieris brassicae*. J. Exp. Bot. 65, 2203–2217. https://doi.org/10.1093/jxb/eru096.

Quiel, J.A., Bender, J., 2003. Glucose conjugation of anthranilate by the *Arabidopsis* UGT74F2 glucosyltransferase is required for tryptophan mutant blue fluorescence. J. Biol. Chem. 278, 6275–6281. https://doi.org/10.1074/jbc.M211822200.

Ross, J., Li, Y., Lim, E., Bowles, D.J., 2001. Higher plant glycosyltransferases. Genome Biol. 2. https://doi.org/10.1186/gb-2001-2-2-reviews3004 reviews3004.

Shi, C.Y., Yang, H., Wei, C.L., Yu, O., Zhang, Z.Z., Jiang, C.J., Sun, J., Li, Y.Y., Chen, Q., Xia, T., Wan, X.C., 2011. Deep sequencing of the *Camellia sinensis* transcriptome revealed candidate genes for major metabolic pathways of tea-specific compounds. BMC Genom. 12, 131. https://doi.org/10.1186/1471-2164-12-131.

Tognetti, V.B., Van Aken, O., Morreel, K., Vandenbroucke, K., van de Cotte, B., De Clercq, I., Chiwocha, S., Fenske, R., Prinsen, E., Boerjan, W., Genty, B., Stubbs, K.A., Inzé, D., Van Breusegem, F., 2010. Perturbation of indole-3-butyric acid homeostasis by the UDP-glucosyltransferase UGT74E2 modulates *Arabidopsis* architecture and water stress tolerance. Plant Cell 22, 2660–2679. https://doi.org/10.1105/tpc.109.071316.

Trapnell, C., Pachter, L., Salzberg, S.L., 2009. TopHat: discovering splice junctions with RNA-seq. Bioinformatics 25, 1105–1111. https://doi.org/10.1093/bioinformatics/btp120.

Veitch, N.C., Grayer, R.J., 2008. Flavonoids and their glycosides, including anthocyanins. Nat. Prod. Rep. 25, 555–611. https://doi.org/10.1039/b718040n.

Wang, J., Hou, B.-k., 2009. Glycosyltransferases: key players involved in the modification of plant secondary metabolites. Front. Biol. China 4, 39–46. https://doi.org/10.1007/s11515-008-0111-1.

Wilson, A.E., Tian, L., 2019. Phylogenomic analysis of UDP-dependent glycosyltransferases provides insights into the evolutionary landscape of glycosylation in plant metabolism. Plant J. 100, 1273–1288. https://doi.org/10.1111/tpj.14514.

War, A.R., Paulraj, M.G., Hussain, B., Buhroo, A.A., Ignacimuthu, S., Sharma, H.C., 2013. Effect of plant secondary metabolites on legume pod borer, *Helicoverpa armigera*. J. Pest. Sci. 86, 399–408. https://doi.org/10.1007/s10340-013-0485-y.

Yang, C., Tian, F., Ma, J., Chen, M., Shi, X., Chen, D., Xie, Y., Zhou, X., Zhou, Z., Dai, X., Xia, T., Gao, L., 2023a. Glycosylation of secondary metabolites: a multifunctional UDP-glycosyltransferase, CsUGT74Y1, promotes the growth of plants. J. Agric. Food Chem. 71, 18999–19009. https://doi.org/10.1021/acs.jafc.3c05843.

Yang, Q., Zhang, Y., Qu, X., Wu, F., Li, X., Ren, M., Tong, Y., Wu, X., Yang, A., Chen, Y., Chen, S., 2023b. Genome-wide analysis of UDP-glycosyltransferases family and identification of UGT genes involved in abiotic stress and flavonol biosynthesis in *Nicotiana tabacum*. BMC Plant Biol. 23, 204. https://doi.org/10.1186/s12870-023-04208-9.

Yoo, S.D., Cho, Y.H., Sheen, J., 2007. Arabidopsis mesophyll protoplasts: a versatile cell system for transient gene expression analysis. Nat. Protoc. 2, 1565–1572. https://doi.org/10.1038/nprot.2007.199.

Zhang, Q., Liu, M., Ruan, J., 2017. Metabolomics analysis reveals the metabolic and functional roles of flavonoids in light-sensitive tea leaves. BMC Plant Biol. 17, 64. https://doi.org/10.1186/s12870-017-1012-8.

Zhao, M., Cai, B., Jin, J., Zhang, N., Jing, T., Wang, J., Pan, Y., Zhou, Z., Zhao, Y., Feng, Y., Yu, F., Zhang, M., Li, Y., Liu, Z., Song, C., 2020a. Cold stress-induced glucosyltransferase CsUGT78A15 is involved in the formation of eugenol glucoside in *Camellia sinensis*. Horticultural Plant Journal 6, 439–449. https://doi.org/10.1016/j.hpj.2020.11.005.

Zhao, M., Jin, J., Wang, J., Gao, T., Luo, Y., Jing, T., Hu, Y., Pan, Y., Lu, M., Schwab, W., Song, C., 2022. Eugenol functions as a signal mediating cold and drought tolerance via UGT71A59-mediated glucosylation in tea plants. Plant J. 109, 1489–1506. https://doi.org/10.1111/tpj.15647.

Zhao, M., Zhang, N., Gao, T., Jin, J., Jing, T., Wang, J., Wu, Y., Wan, X., Schwab, W., Song, C., 2020b. Sesquiterpene glucosylation mediated by glucosyltransferase UGT91Q2 is involved in the modulation of cold stress tolerance in tea plants. New Phytol. 226, 362–372. https://doi.org/10.1111/nph.16364.

Zhao, X., Wang, P., Li, M., Wang, Y., Jiang, X., Cui, L., Qian, Y., Zhuang, J., Gao, L., Xia, T., 2017. Functional characterization of a new tea (*Camellia sinensis*) flavonoid glycosyltransferase. J. Agric. Food Chem. 65, 2074–2083. https://doi.org/10.1021/acs.jafc.6b05619.

Zhang, J., Zhang, X., Ye, M., Li, X.W., Lin, S.B., Sun, X.L., 2020. The jasmonic acid pathway positively regulates the polyphenol oxidase- based defense against tea geometrid caterpillars in the tea plant (*Camellia sinensis*). J. Chem. Ecol. 46, 308–316. https://doi.org/10.1007/s10886-020-01158-6.

Zhu, J., Chen, H., Liu, L., Xia, X., Yan, X., Mi, X., Liu, S., Wei, C., 2024. JA-mediated MYC2/LOX/AOS feedback loop regulates osmotic stress response in tea plant. Horticultural Plant Journal 10, 931–946. https://doi.org/10.1016/j.hpj.2022.10.014.

Zhu, J., Wang, X., Guo, L., Xu, Q., Zhao, S., Li, F., Yan, X., Liu, S., Wei, C., 2018. Characterization and alternative splicing profiles of the lipoxygenase gene family in tea plant (*Camellia sinensis*). Plant Cell Physiol. 59, 1765–1781. https://doi.org/10.1093/pcp/pcy091.